

Silver Ions and Quantum-Sized Silver Sulfide Clusters in Zeolite A

Dominik Brühwiler, Claudia Leiggner and Gion Calzaferri*

University of Bern, Department of Chemistry and Biochemistry
Freiestrasse 3, CH-3012 Bern, Switzerland

* e-mail: gion.calzaferri@iac.unibe.ch

UV/vis spectroscopic studies of $\text{Ag}^+_{x}\text{Na}^+_{12-x}\text{A}$, $\text{Ag}^+_{x}\text{Ca}^{2+}_{6-0.5x}\text{A}$, and $\text{Ag}^+_{9.5}\text{ZK-4}$ in conjunction with molecular orbital calculations lead to the result that 4-ring coordinated Ag^+ is responsible for the deep yellow color observed in silver loaded zeolite A activated at room temperature. The electronic transitions can be interpreted as charge transfer from zeolite oxygen lone pairs to Ag^+ . We therefore denote them as $5s(\text{Ag}^+) \leftarrow n(\text{O})$ LMCT. The reaction of H_2S with activated Ag^+ -loaded zeolite A leads to the formation of quantum-sized, luminescent silver sulfide clusters inside the zeolite cavities. The cluster size can be varied by adjusting the initial silver loading.

1. SILVER IONS IN ZEOLITE A

Rálek et al. reported in 1962 that hydrated colorless zeolite $\text{Ag}^+_{x}\text{Na}^+_{12-x}\text{A}$ turns yellow to red on activation.[1] No explanation of this phenomenon was given at that time. Later it was believed that the color change was due to the formation of silver clusters (Ag_n^0) in the cavities of the zeolite. These neutral silver species were assumed to form at elevated temperature via an autoreduction process in which O_2 from the zeolite framework was released.[2] We recently showed that activation at room temperature under high vacuum is sufficient to produce the yellow form of $\text{Ag}^+_{x}\text{Na}^+_{12-x}\text{A}$.[3] The fully reversible color change which depends on the hydration state of the silver zeolite was attributed to electronic charge transfer transitions from the oxygen lone pairs of the zeolite framework to the empty 5s orbitals of the silver ions. In activated silver zeolite A materials, the silver ions are forced to coordinate zeolite oxygen because an insufficient number of water molecules are available. The question remained whether specific coordination sites which act as yellow and/or red color centers can be identified.

1.1. Experimental Observations[3,4]

UV/vis spectra of hydrated and activated $\text{Ag}^+_{x}\text{Na}^+_{12-x}\text{A}$, $\text{Ag}^+_{x}\text{Ca}^{2+}_{6-0.5x}\text{A}$, and $\text{Ag}^+_{9.5}\text{ZK-4}$ materials were studied. The marked site preference of the ions in $\text{Ag}^+_{x}\text{Ca}^{2+}_{6-0.5x}\text{A}$, probed by gas adsorption experiments, was found to offer the unique possibility of investigating different coordination sites of Ag^+ in zeolite A.

Pure sodium and calcium zeolite A are colorless in both their hydrated and their activated states. They do not absorb light within the spectral range from 200 to 1000 nm. This means that any absorption band in this range observed in silver zeolite A materials is due to the presence of silver ions. Our observations lead to the result that Ag^+ coordinated to 6- or 8-ring oxygens gives rise to electronic transitions in the near-UV region. Only Ag^+ coordinated to 4-ring oxygens leads to the 450 nm absorption responsible for the typical deep yellow color. We have also observed that Ag^+ avoids the 4-ring sites in $\text{Ag}^+_{x}\text{Ca}^{2+}_{6-0.5x}\text{A}$ as long as x is smaller than 10. In the case of $\text{Ag}^+_{x}\text{Na}^+_{12-x}\text{A}$, either a sodium or a silver ion is forced to occupy a 4-ring site. The presence of the 450 nm band for a loading of $x = 0.2$ proves that isolated silver ions are

sufficient to cause such an absorption and that the 4-ring coordination of Ag^+ is significantly stronger than that of Na^+ .

The red color of elevated temperature activated samples is caused by a strong absorption band at 520 nm. We observed that samples which remained colorless after room temperature activation never turned red, that samples with lower silver content than one Ag^+ per pseudo unit cell did not turn red, and that room temperature dehydration under our experimental conditions was not sufficient to produce red colored samples. This indicates that only samples with 4-ring coordinated Ag^+ and an adjacent Ag^+ on a 6-ring site can give rise to the 520 nm band. A thorough dehydration is necessary in order to enforce the interaction between those two silver ions, which leads to the generation of a lower lying state giving rise to the red color.

Yellow and red colored materials turn colorless again, when exposed to humidity. The reversibility is complete for the yellow samples while a broad but weak absorption in the near-UV remains after rehydration of the red samples.

1.2. Theoretical Considerations[4]

Molecular orbital calculations [5] carried out on a sufficiently large zeolite part, obtained by fusing eight α -cages at 8-rings, allowed us to address questions about the nature of the HOMO and of the LUMO region, about the contributions of the zeolite framework atoms to the electronic transitions, about the influence of the local symmetry of Ag^+ at 4- and 6-ring sites, and about the importance of Ag^+-Ag^+ interactions. In order to avoid geometries without experimental relevance, we restricted this study to Ag^+ at 4- and 6-ring sites known from X-ray measurements.[6] The following results were obtained on the anhydrous state (see ref 7 for a discussion of the water to silver LMCT transitions). We found that the occupied frontier orbital region consists mainly of two bunches of levels: the HOMO region from about -11 to -12.6 eV and the next levels below -13.6 eV. The LUMO consists of a single level of mainly 5s(Ag) character. The LUMO+1 was found to be energetically too high to be of relevance in this study. Thus, the oscillator strength of transitions from the first 1244 levels to the LUMO were calculated (see ref 4 for computational details).

For 6-ring coordinated Ag^+ all levels in the HOMO region derive from mostly noninteracting oxygen lone pairs which we abbreviate as n(O). The LUMO is a rather pure 5s(Ag), thus all electronic excitations in question are LMCT transitions from oxygen lone pairs of the zeolite framework to Ag^+ . We denote such electronic transitions as $5s(\text{Ag}^+) \leftarrow n(O)$. They are energetically located in the near-UV and depend only little on the polarization.

The bands of the 4-ring coordinated Ag^+ are strongly polarized. Two almost degenerate low-energy absorption bands and a prominent high-energy band dominate the spectrum. The former can be described as a $5s(\text{Ag}^+) \leftarrow n(O)$ LMCT transition. It is responsible for the yellow color of activated silver loaded zeolite A.

2. QUANTUM-SIZED SILVER SULFIDE CLUSTERS

The low-temperature phase of bulk silver sulfide ($\alpha\text{-Ag}_2\text{S}$ or acanthite, stable up to 450 K) is a semiconductor with a monoclinic structure and a band gap of approximately 1 eV at room temperature and 1.4 eV at 0 K.[8] Bulk silver sulfide has been considered for photoimaging and photodetection in the IR region [9], while molecules and small clusters are known to play an important role in photographic sensitivity.[10-14] In contrast to the thoroughly investigated nanoparticles of semiconductors such as CdS [15] or ZnS [16], only a few studies on clusters of Ag_2S are currently available.[17-21] Silver sulfide nanoparticles show a strong tendency to aggregate into bulk, which renders the preparation of small clusters extremely difficult. By using the well-defined cavities of zeolite A, we developed a method of synthesizing silver sulfide clusters in the size regime below 15 Å.[22] The preparation is based on the observation that Ag^+ -loaded zeolite A can be reversibly activated at room temperature (see chapter 1).[3] Its reaction with H_2S leads to the formation of silver sulfide clusters inside the zeolite cages. The cluster size can be varied by adjusting the initial amount of exchanged silver ions.

The predominant electronic transition in bulk Ag_2S and presumably also in Ag_2S nanoparticles is a charge transfer from 3p(S) to 5s(Ag). Figure 1 shows the calculated density of states (DOS) of bulk $\alpha\text{-Ag}_2\text{S}$. The contribution of 3p(S) states to the valence band is much more pronounced than for the conduction band, which is mainly of 5s(Ag) character. An analogous observation can be made for a hypothetical Ag_2S molecule. Furthermore the HOMO-LUMO region of such a molecule, and most probably also of larger silver sulfide clusters, fits well into the energy gap between the oxygen lone pairs of the zeolite A framework and the zeolite A LUMO region, therefore allowing the investigation of its electronic transitions.

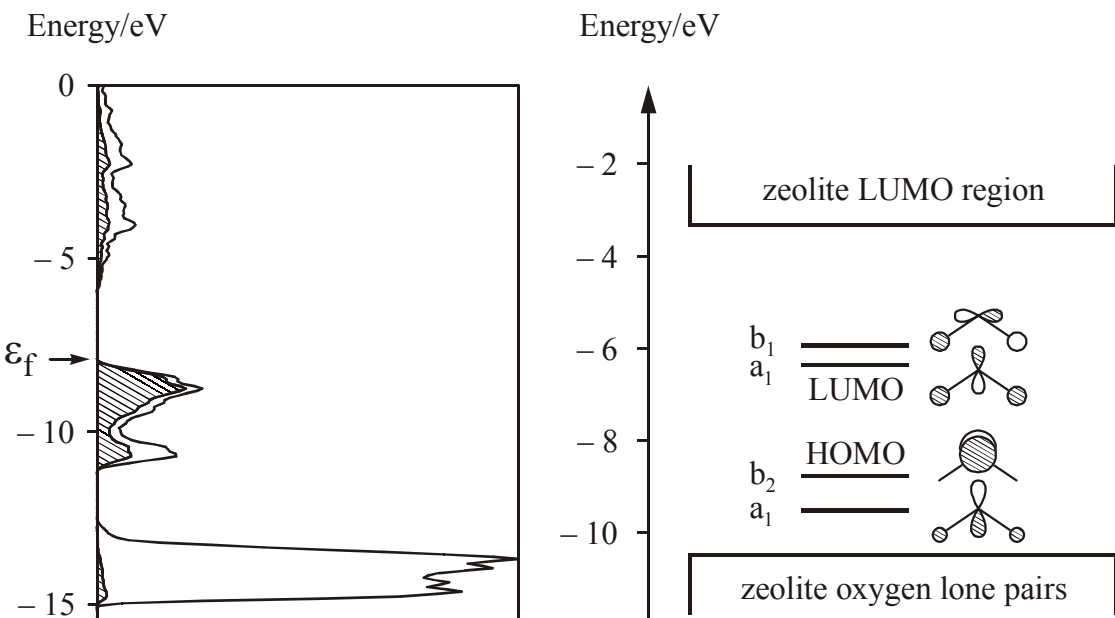


Fig. 1. Left: Density of states (DOS) plot of $\alpha\text{-Ag}_2\text{S}$. The hatched region indicates the contribution of sulfur 3p-states (BICON-CEDiT [23] calculation). The Fermi level ϵ_f is marked by an arrow. Right: HOMO-LUMO region of a hypothetical Ag_2S molecule in comparison to the HOMO-LUMO region of zeolite A (ICON-EDiT [5] calculation).

In our synthesis of quantum-sized silver sulfide clusters, the zeolite is used as a stabilizing matrix which prevents the silver sulfide particles from growing and aggregating into bulk. Clusters were synthesized in sodium zeolite A (NaA) and calcium zeolite A (CaA). Zeolite A microcrystals of high purity were prepared according to ref 24. The properties of the silver sulfide zeolite A composites depend strongly on the silver sulfide loading density. We have shown that increasing the silver sulfide content leads to the formation of larger clusters and to a drastic variation of the optical absorption and luminescence of the material.[22] The color of the hydrated silver sulfide zeolite A composites ($\text{Ag}_2\text{S}-\text{NaA}-x$ or $\text{Ag}_2\text{S}-\text{CaA}-x$, where x denotes the average number of silver ions per α -cage) ranges from colorless ($0.01 < x < 0.5$) to yellow-green ($0.5 < x < 2$) to brown ($x > 2$) (see Figure 2).

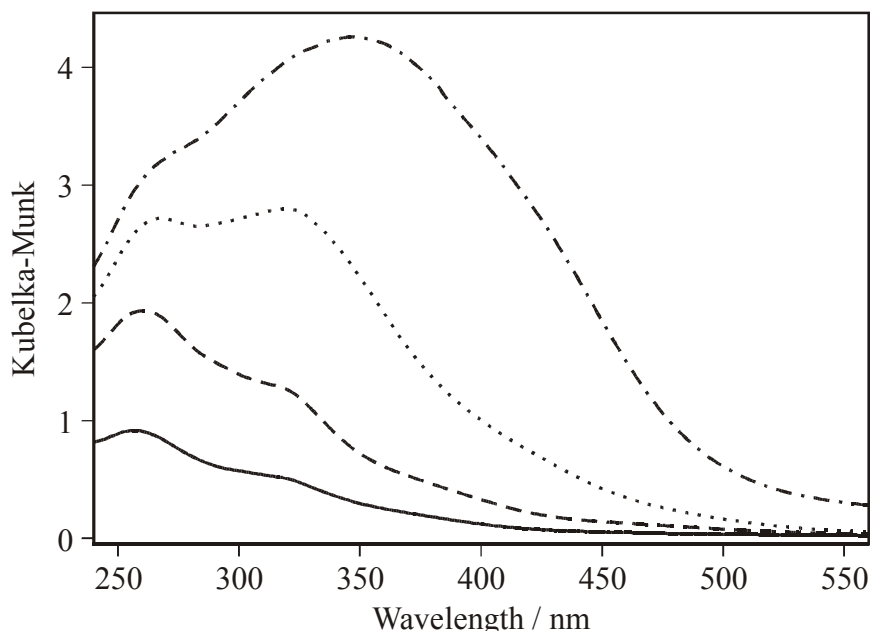


Fig. 2. Diffuse reflectance spectra of hydrated $\text{Ag}_2\text{S}-\text{NaA}-0.05$ (solid), $\text{Ag}_2\text{S}-\text{NaA}-0.1$ (dash), $\text{Ag}_2\text{S}-\text{NaA}-0.5$ (dot) and $\text{Ag}_2\text{S}-\text{NaA}-2$ (dash-dot) under ambient conditions.

The silver sulfide zeolite A composites exhibit a variety of luminescence properties depending on the silver sulfide loading density and to a smaller extent on the co-cations. A low silver sulfide content is basically characterized by a blue-green emission and distinct absorption bands, while samples with medium silver sulfide content show an orange-colored emission and a continuous absorption (see Figure 3). Further increasing the silver sulfide content ($x > 2$) and therefore the cluster size results in a bathochromic shift of this characteristic emission and a gradual shortening of the luminescence decay times. The decays are multiexponential (in the microsecond range at 110 K) owing to silver sulfide clusters on different sites inside the zeolite cages and/or a narrow size distribution. The determination of the actual cluster sizes and structures is therefore a difficult task. Given the dimensions of the α -cage, the stoichiometry of the largest cluster that would fit in such a cavity is approximately Ag_8S_4 . In the case of high silver sulfide loadings (as in $\text{Ag}_2\text{S}-\text{CaA}-6$) we expect the formation of superclusters through interactions between clusters in adjacent cavities.

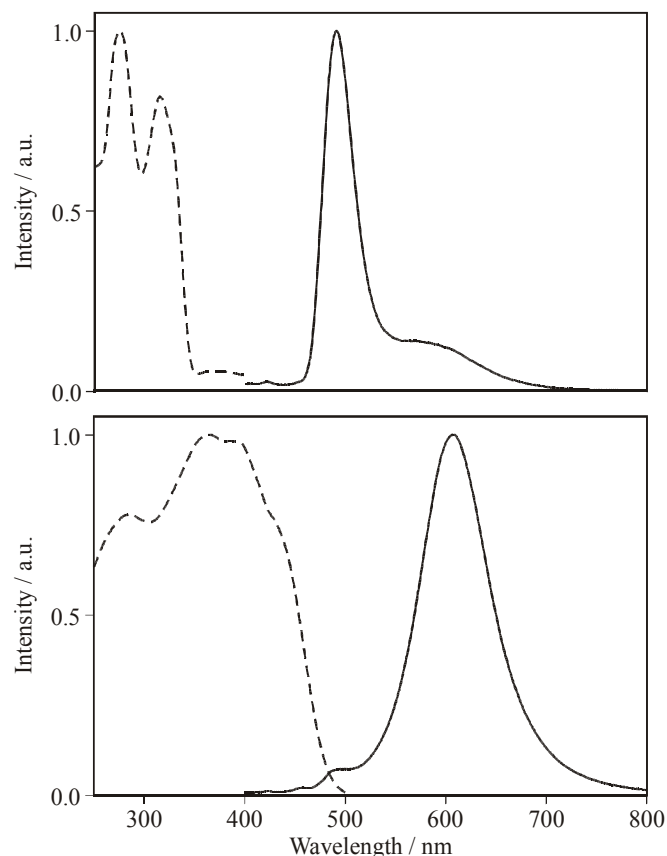


Fig. 3. Luminescence spectra (solid lines, excitation at 280 nm) and excitation spectra (dashed lines) of hydrated Ag_2S -CaA-0.01 (top) and Ag_2S -CaA-2 (bottom) at 80 K.[25]

3. CONCLUSIONS

UV/vis spectroscopic studies of $\text{Ag}^+_{x}\text{Na}^{+}_{12-x}\text{A}$, $\text{Ag}^+_{x}\text{Ca}^{2+}_{6-0.5x}\text{A}$, and $\text{Ag}^+_{9.5}\text{ZK-4}$ in conjunction with molecular orbital calculations lead to the result that 4-ring coordinated Ag^+ is responsible for the yellow color observed in silver loaded zeolite A activated at room temperature. The transition is a charge transfer from zeolite oxygen lone pairs to the empty 5s orbitals of Ag^+ . The room temperature activation of zeolite A containing silver ions is completely reversible. It is therefore possible to synthesize silver sulfide clusters inside the zeolite cavities by reaction with H_2S . The cluster size and thus the spectroscopic properties (absorption, luminescence) of the material can be varied by adjusting the initial silver loading. The silver sulfide zeolite A composites are expected to yield valuable insight into the still relatively unknown chemical and physical properties of small silver sulfide species.

REFERENCES

1. M. Rálek, P. Jíru, O. Grubner and H. Beyer, *Collect. Czech. Chem. Commun.*, 27 (1962) 142.
2. T. Sun and K. Seff, *Chem. Rev.*, 94 (1994) 857.
3. R. Seifert, A. Kunzmann and G. Calzaferri, *Angew. Chem., Int. Ed. Engl.*, 37 (1998) 1521.
4. R. Seifert, R. Rytz and G. Calzaferri, *J. Phys. Chem. A*, 104 (2000) 7473.
5. R. Rytz, S. Glaus, M. Brändle, D. Brühwiler and G. Calzaferri, ICON-EDiT, Extended Hückel Molecular Orbital and Transition Dipole Moment Calculations, <http://iacrs1.unibe.ch>, Department of Chemistry and Biochemistry, University of Bern, Freiestrasse 3, 3012 Bern, Switzerland, 2000.
6. L. R. Gellens, J. V. Smith and J. J. Pluth, *J. Am. Chem. Soc.*, 105 (1983) 51.
7. S. Glaus and G. Calzaferri, *J. Phys. Chem. B*, 103 (1999) 5622.
8. P. Junod, H. Hediger, B. Kilchör and J. Wullschleger, *Philos. Mag.*, 36 (1977) 941.
9. S. Kitova, J. Eneva, A. Panov and H. Haefke, *J. Imaging Sci. Technol.*, 38 (1994) 484.
10. K. Kuge and N. Mii, *J. Imaging Sci. Technol.*, 33 (1989) 83.
11. J. W. Mitchell, *J. Imaging Sci. Technol.*, 42 (1998) 215.
12. E. Charlier, M. Van Doorselaer, R. Gijbels, R. De Keyzer and I. Geuens, *J. Imaging Sci. Technol.*, 44 (2000) 235.
13. T. Tani, *J. Imaging Sci. Technol.*, 39 (1995) 386.
14. R. Baetzold, Proc. IS&T/SPSTJ's International Symposium on Silver Halide Imaging: "Silver Halide in a New Millennium", Sainte-Adele, Quebec, Canada, 2000, p. 82.
15. T. Vossmeyer, L. Katsikas, M. Giersig, I. G. Popovic, K. Diesner, A. Chemseddine, A. Eychmüller and H. Weller, *J. Phys. Chem.*, 98 (1994) 7665.
16. J. Nanda, S. Sapra, D. D. Sarma, N. Chandrasekharan and G. Hodes, *Chem. Mater.*, 12 (2000) 1018.
17. L. Motte and M. P. Pilani, *J. Phys. Chem. B*, 102 (1998) 4104.
18. V. M. Belous, V. I. Tolstobrov, O. I. Sviridova and K. V. Chibisov, *Dokl. Phys. Chem. (Engl. Transl.)*, 262 (1982) 75.
19. K. Akamatsu, S. Takei, M. Mizuhata, A. Kajinami, S. Deki, S. Takeoka, M. Fujii, S. Hayashi and K. Yamamoto, *Thin Solid Films*, 359 (2000) 55.
20. Y. Sun, J. E. Riggs, H. W. Rollins and R. Guduru, *J. Phys. Chem. B*, 103 (1999) 77.
21. M. C. Brelle, J. Z. Zhang, L. Nguyen and R. K. Mehra, *J. Phys. Chem. A*, 103 (1999) 10194.
22. D. Brühwiler, R. Seifert and G. Calzaferri, *J. Phys. Chem. B*, 103 (1999) 6397.
23. M. Brändle, R. Rytz and G. Calzaferri, BICON-CEDiT, Extended Hückel Band Structure and Transition Dipole Moment Calculations, <http://iacrs1.unibe.ch>, Department of Chemistry and Biochemistry, University of Bern, Freiestrasse 3, 3012 Bern, Switzerland, 2000.
24. P. Lainé, R. Seifert, R. Giovanoli and G. Calzaferri, *New J. Chem.*, 21 (1997) 453.
25. G. Calzaferri, D. Brühwiler, S. Glaus, D. Schürch, A. Currao and C. Leiggner, *J. Imaging Sci. Technol.*, 45 (2001) 331